Polymer 50 (2009) 250–260

Contents lists available at ScienceDirect

Polymer

journal homepage: www.elsevier.com/locate/polymer

Ultrasound assisted twin screw extrusion of polymer–nanocomposites containing carbon nanotubes

A.I. Isayev*, Rishi Kumar, Todd M. Lewis

Institute of Polymer Engineering, The University of Akron, Akron, OH 44325-0301, USA

ARTICLE INFO

Article history:
Received 31 May 2008
Received in revised form
21 October 2008
Accepted 23 October 2008
Available online 8 November 2008

Keywords:
Polyetherimide
Multi-walled carbon nanotubes
Ultrasound

ABSTRACT

The unique morphology and strong intertube attraction between carbon nanotubes (CNTs) make the dispersion of CNTs challenging and hence limit its effective use. A novel method for the continuous dispersion of multi-walled carbon nanotubes (MWNTs) in a polymer matrix for manufacturing high performance nanocomposites was developed using an ultrasonically assisted twin screw extrusion process. Reduction of the die pressure and variation of the ultrasonic power consumption as a function of amplitude were measured at various MWNT loadings. The effect of ultrasound on rheological, electrical, morphological and mechanical properties of polyetherimide (PEI) matrix and PEI-filled with 1–10 wt% MWNTs was studied. In the treated nanocomposites, the complex viscosity, storage and loss moduli were increased and damping characteristics were decreased as compared to untreated ones. Rheological and electrical percolations were found to be between 1 and 2 wt% MWNT loading. Ultrasonic treatment does not affect the electrical conductivity of nanocomposites. Mechanical properties such as Young's modulus and tensile strength were significantly increased with MWNT loading but moderately with ultrasonic treatment at high loadings and certain ultrasonic amplitudes. The morphology and state of dispersion of MWNTs were investigated by means of HRSEM. In the ultrasonically treated nanocomposites, the obtained micrographs showed excellent dispersion of MWNTs in PEI matrix.

1. Introduction

High performance fiber-reinforced composites have been widely used in various engineering applications due to their lightweight and high mechanical properties. Till date, carbon–fiber and glass–fiber composites dominate the industry. There are some limitations associated with the glass–fiber-reinforced composites such as the accumulation of electrostatic charge on their surface which can cause local heating resulting in the catastrophic failure of the surrounding materials. In recent years [1], the polymer/CNT composites have gained tremendous attention in both academia and industry. While the first image resembling nanotubes was published in 1976 [2], major advances in the area happened after the formation of MWNTs was published by Iijima in 1991 [3]. Because of the high aspect ratio (100–1000) of MWNTs and exceptional electrical properties along with their lightweight [4,5], it is possible to achieve the percolation threshold at very low loadings [6]. The biggest challenge in effectively using MWNTs is their lack of dispersion in a polymer matrix. During synthesis of MWNTs, nanotubes easily aggregate or form bundles due to strong intertube van der Waals attraction and hence limit the effective use of their exceptional properties obtained at the individual nanotube level. Many researchers [7,8] have tried different routes to disperse MWNTs. However, successful dispersion still remains a challenge as can be seen from the recent reviews on dispersion of MWNTs in a polymer matrix [9,10]. Current methods commonly used for the dispersion of nanotubes in a polymer matrix are: in-situ polymerization, mechanical and chemical treatment [10]. Among these methods in-situ polymerization and chemical modification may not be commercially viable due to their limitation in scale up and their negative environmental impact. Prolonged sonication of the MWNTs in an ultrasonic bath using solvent is one of the most commonly used methods to disperse nanotubes. However, it introduces defects in MWNTs and results in reduced aspect ratios which is the basis for many of their attractive properties [11].

Melt processing is more efficient, rapid and environmentally friendly method to disperse MWNTs in a polymer matrix. It is one of the most preferred techniques from an industrial application point of view because it can easily be scaled up. A number of studies have been done on melt processing/extrusion of polymer/CNT composites [12–16]. In one study [12], a miniature mixer was used to mix PMMA with up to 26 wt% MWNT loading. The extruded melt was then compression molded to make thin films. Dynamic mechanical behavior shows a significant increase in the storage modulus of thin film samples. Morphological, rheological and electrical studies on PC/MWNT composites were also carried out

* Corresponding author. Tel.: +1 330 972 6673.
E-mail address: aisayev@uakron.edu (A.I. Isayev).

0032-3861/$ – see front matter © 2008 Elsevier Ltd. All rights reserved.
doi:10.1016/j.polymer.2008.10.052

indicating electrical percolation at loadings between 1 and 2 wt% [13,14]. Also, HDPE/MWNT composites were studied and an electrical percolation near 7.5 wt% loading was found which is higher than that normally observed for other polymers [15]. However, no significant improvement in mechanical properties was observed.

Functionalized MWNTs were prepared and mixed with Nylon 6 and then further processed in an internal mixer [16]. A significant improvement in Young's modulus and tensile strength of Nylon 6 was observed at a 2 wt% MWNT loading. In another study [17], PEI/SWNT composites were prepared in a single screw extruder. No significant improvement in mechanical properties was observed for thin film samples. However, significant increase in the tensile modulus was observed when the extruded melt was drawn into thin fibers. From the above discussion, there is a clear need to develop a new method which is rapid, clean and commercially viable.

Over the past decade extensive work has been done to develop a novel extrusion process with the aid of high power ultrasound [18,19]. A number of studies [20–22] on the effect of ultrasound on polymers have been published and reported in various articles. It was shown that ultrasonic oscillations can breakdown the 3-D network in vulcanized rubber within seconds. Ultrasound was also found to improve the compatibilization of immiscible plastic blends, plastic/rubber and rubber/rubber blends during this process [23]. In recent years, the use of ultrasound to disperse nanofiller in a polymer matrix is gaining attention. Ultrasound helps in rapid intercalation and partial exfoliation of nano-clay in a polymer matrix [24].

To our knowledge, there has been no work done to improve the dispersion of CNTs in polyimide matrix with the help of ultrasound assisted extrusion process. This work presents a novel method and apparatus for the continuous dispersion of CNTs in a polymer matrix. In particular, an ultrasound assisted twin screw extruder was developed and the compounding of the PEI/MWNT was carried out. PEI was chosen because of its extensive use in composites for various industrial applications due to its desirable combination of mechanical and thermal properties. Moreover, PEI has desired processability and outstanding dimensional and thermo-oxidative stability. The effects of ultrasound on die pressure, electrical conductivity, rheological, morphological and mechanical properties were studied.

2. Experimental

2.1. Materials

Polyetherimide (PEI) in powder form made by GE Plastics (Pittsfield, MA) under trade name ULTEM 1000P was used as received. The MWNTs were provided by Nanostructured & Amorphous Materials, Houston, TX, and were used as received. The MWNTs had an outside diameter of 10–20 nm with lengths of 0.5–200 μm.

2.2. Nanocomposite preparation

The PEI powder was mixed prior to processing with 1, 2, 5, and 10 wt% MWNT loadings by ball milling for 24 h. The mixture was then dried for a minimum of 24 h at 110 °C in a vacuum oven prior to processing. For melt processing, a commercially available continuous co-rotating intermeshing twin screw micro-extruder (PRISM USA LAB 16, Thermo Electron Corp., UK) having a diameter of 16 mm with a $L/D = 25$ was used. It was modified by addition of ultrasonic treatment sections at the exit of the micro-extruder as shown in Fig. 1. The ultrasonic slit die of $4.5 \times 0.75 \times 0.157$ in^3 dimension was designed and connected to the micro-extruder through a die connector.

A pair of 800 W ultrasonic power supply (Branson Ultrasonics Corp., CT) generated ultrasound at 40 kHz frequency. Each ultrasonic power supply is connected in series to a converter (Branson Ultrasonic Corp., CT), 1:1 booster (Branson Ultrasonics Corp., CT) and the water cooled titanium horns which are in direct contact with the polymer melt. The horns provide the longitudinal vibrations in the direction perpendicular to the flow direction. Both horns were symmetrically mounted on the slit die and both were operated simultaneously for all ultrasonically treated samples. The

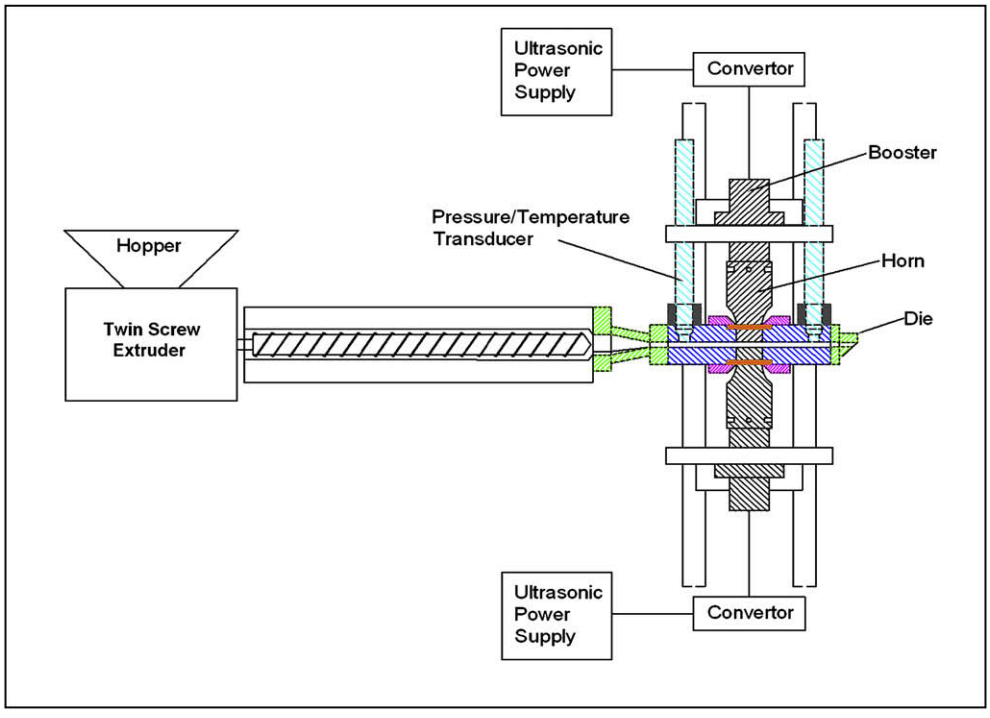

Fig. 1. The ultrasonic twin screw micro-extruder.

ultrasonic horns have square cross section with 19.05×19.05 mm^2 (0.75×0.75 in^2) tip area. The imposition of high intensity ultrasonic waves on the flowing polymer melt was digitally controlled from the ultrasonic power supplies. The horn tips were calibrated in air for ultrasonic amplitude in the range of 0–8 μm. A range of ultrasonic amplitude varying from 0 to 6.0 μm were applied to molten compound to study the effect of increasing ultrasonic power on the dispersion of the CNTs in a polymer melt.

The gap size between the horns creates a channel with clearance of 4 mm for flow of polymer melt. 40% by weight graphite filled polyimide (Vespel SP-22) seals were used to prevent the flow of polymer melt along the side of the horn in the ultrasonic treatment zone.

Heating elements were installed on slit die and on the transition part connecting the micro-extruder with the slit die. Temperature controllers and thermocouples were used together with the heating elements to allow die temperature and die connector temperature to go from room temperature to 400 °C during extrusion.

Two pressure transducers (TPT 412-5M-6/18, Dynisco Instruments, Franklin, MA) of maximum pressure of 5000 psi, to measure the melt temperature and pressure, were placed in the slit die zone immediately before and after the ultrasonic treatment zone. The pressure, temperature and power consumption were recorded by data acquisition system (Dataq Instruments, DI-715-U, Akron, OH).

The temperature in the barrel section was set from feed zone to die zone as 280 °C, 340 °C, 350 °C, 360 °C, 360 °C. The temperatures were digitally controlled by several heaters connected to temperature controllers. The screw speed was set at 50 rpm. A feed rate of 0.5 lb/h was controlled by a feeder (Brabender Technology MT-2, Germany). The mean residence time of the melt in the ultrasonic treatment zone was 29 s. The extrudate was collected, dried and pelletized in a grinder (Weima America Inc., Fort Mill, SC).

Tensile bars according to ASTM D-638 were prepared using the mini-jet piston injection molder (HAAKE, Thermo Electron Corp., Germany) at a melt temperature of 360 °C, a mold temperature of 130 °C and injection pressure of 740 bars. High temperature mold release agent (Frekote HMT2) was sprayed on the heated mold before injecting the material. Prepared nanocomposites were compression molded into discs of 25 mm diameter and 2.2 mm thickness at 300 °C using a compression molding press (CARVER 4122, Wabash, IN) for the rheological measurements. The samples for electrical conductivity measurement were also compression molded into discs of 90 mm diameter and 1 mm thickness. For compression molding samples, metal plates and mold were sprayed with high temperature mold release agent and Kapton® polyimide film (Dupont) was placed between the metal plates and the mold.

2.3. Rheological measurements

The rheological properties of the nanocomposites were studied using an advanced rheometric expansion system (Model ARES LS, TA Instruments). A 25 mm parallel plate geometry in the oscillatory shear mode with dynamic frequency sweep test was used at 340 °C and a fixed strain amplitude of 2%. The frequency range was 0.03–100 rad/s. The material was placed between the heated parallel plates and squeezed and then excess material was removed from the sides to avoid any boundary effects. The dynamic measurements provide information about nanocomposites in their original state without destroying their structure, as would occur in the case of the steady state measurements.

2.4. Electrical resistivity

A Keithley electrometer (Model 6517A, Keithley Instruments, Cleveland, OH) equipped with an 8009 test fixture was used to measure the volume resistivity of the samples in accordance with the ASTM D257 method using applied voltage of 0.1 V. It was difficult to measure the volume resistivity at higher voltages for all the samples since at high CNT loadings, the material becomes highly conductive and it caused the short circuiting in the electrometer. Therefore, the voltage of 0.1 V was selected to measure the volume resistivity of all the nanocomposite samples for comparison. It is due to the fact that the different voltage can lead to different resistivity values as conductivity shows dependence on the applied voltage. The readings were taken 60 s after the applied voltage to get the stabilized values.

2.5. Mechanical properties

Tensile measurements on injection molded samples were carried out using an Instron test machine (Model 5567; Instron Corp., Canton, MA). Tests were carried out according to ASTM D-638 test method at a cross-head speed of 5 mm/min using a 30 kN load cell and an extensometer.

2.6. Morphological study

The state of dispersion of MWNTs in a polymer matrix can be studied by visual inspection of the nanotubes using micrographs obtained by high resolution microscopy. Therefore, microscopic analysis was carried out to study the morphology and state of dispersion of MWNTs in a polymer matrix using field emission high resolution scanning electron microscope (HRSEM, Model JEOL JSM-7401 F, Tokyo, Japan). The cryofractured surfaces of injection molded impact bar specimens without and with silver sputter coating were used for the HRSEM investigation. The image analysis sofware (ImageJ) was used to determine the distribution of diameters of nanotubes from the HRSEM micrographs.

3. Results and discussion

3.1. Process characteristics

Fig. 2 shows the entrance die pressure (a) and power consumption (b) for various loadings of MWNTs as a function of ultrasonic amplitude during the extrusion of PEI/MWNT composites. The pressure is measured before the ultrasonic treatment zone. A continuous decrease in the pressure with increasing ultrasonic amplitude was observed. This could be due to occurrence of acoustic cavitation phenomenon in the melt leading to both permanent and thixotropic changes in the melt. Typically, cavitation can cause the scission of the molecular chains resulting in degradation of the polymers which could be seen from reduction in viscosity. However, no such reduction in viscosity was observed for neat polymer as shown in Fig. 3. So reduction in the die pressure cannot be explained on the basis of degradation of polymer under action of ultrasound but can be attributed to thixotropic changes in the melt. However, it should be noted that due to the presence of MWNTs, degradation of the polymer matrix cannot be completely ruled out since the possibility of a local energy density at the interfaces between polymer and MWNTs exists. In addition to the thixotropic effect produced by ultrasound, the decrease in die pressure is due to heating from dissipated ultrasonic energy, reduction in friction at horn surfaces due to ultrasonic vibrations and possible shear thinning effect created by ultrasound waves. The die pressure increases with the increasing MWNT loading, as expected, due to increase in viscosity caused by an increase in MWNT content. Due to the ultrasonic treatment a tremendous decrease in die pressure at high amplitudes leads to improved processability of polymer melts, allowing one to achieve a faster extrusion rate. In the case of a twin screw extrusion, the higher feed rate will lead to build up of the higher die pressure. Therefore, without imposition of ultrasound the die pressure may become

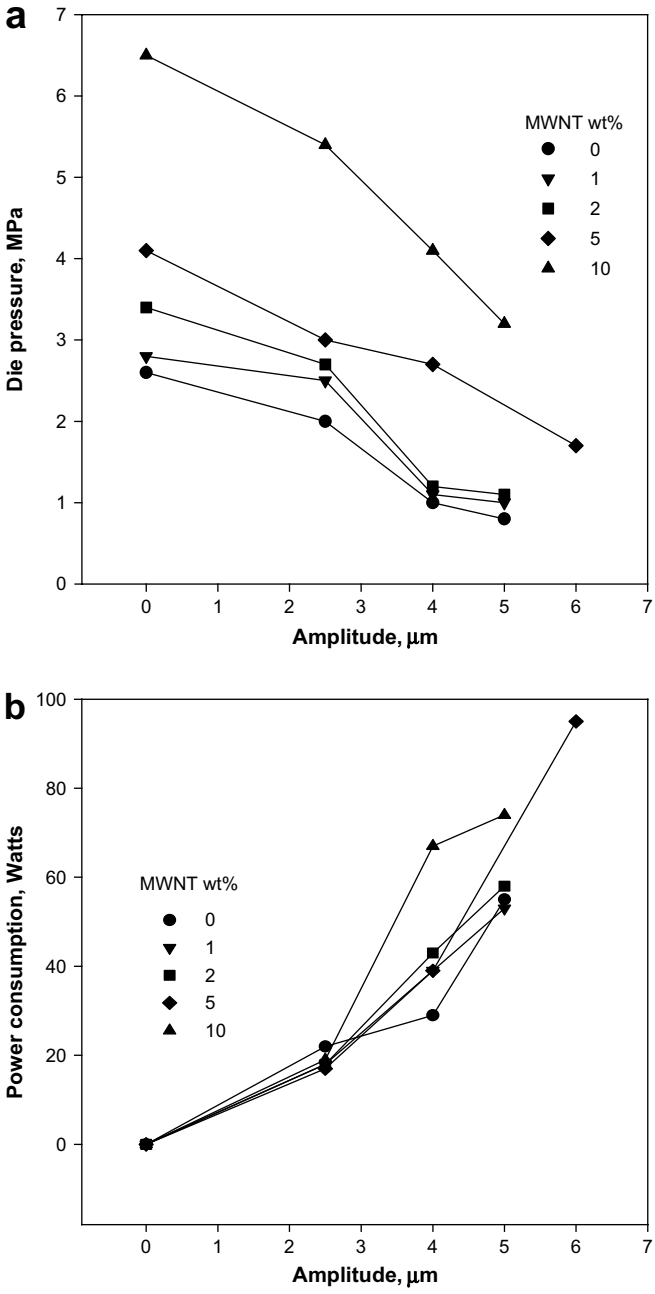

Fig. 2. Die pressure (a) and ultrasonic power consumption (b) versus amplitude at different MWNT loadings.

prohibitively high. However, with imposition of ultrasound the pressure will be reduced allowing one to increase the feed rate.

The measured power consumption, shown in Fig. 2(b), is the total power consumption during the treatment of nanocomposites, a part of which is dissipated as heat and the rest is exerted to disperse nanotubes in melt and potentially increasing the polymer–nanotube interaction. It was observed that power consumption increased with the increase of ultrasonic amplitude and MWNT loading, indicating that more energy was transmitted from the horns to the polymer melt. However, the highest value of power consumption is below 100 W.

3.2. Rheology

The effect of ultrasound on the complex viscosity of nanocomposites as a function of frequency at different MWNT loadings

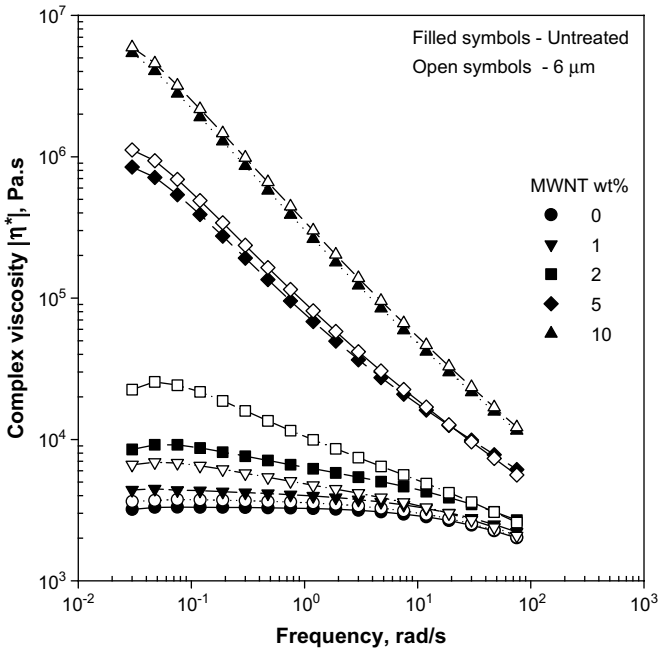

Fig. 3. Complex viscosity as a function of frequency at different MWNT loadings for untreated and ultrasonically treated nanocomposites at an amplitude of 6 μm.

is shown in Fig. 3. There is tremendous increase in the complex viscosity of nanocomposites with the increase of MWNT loadings and ultrasound. However, at high loadings the effect of ultrasound on viscosity is masked by its high value. Viscosity increased by an order of magnitude in comparison with that at low loadings. In other words, the relative change of viscosity at high loadings is less than that at low loadings, but absolute changes are very large. The effect is more pronounced in the low frequency region with minimal increase in the high frequency region. The increase in complex viscosity due to ultrasound is attributed to better dispersion of nanotubes in the polymer matrix with enhanced polymer–nanotube interaction. It has been observed that for low loadings of MWNTs, up to 2 wt%, a Newtonian plateau, similar to that of pure PEI, occurs in the low frequency region. However, this plateau disappears as the MWNT loading is increased beyond 2 wt%. Viscosity increases with MWNT loading and a stronger shear thinning behavior observed at high MWNT loading. This is in accordance with earlier studies done on PC/MWNT [13], HDPE/MWNT [15] and clay-based nanocomposites [25–27]. The increase in viscosity observed in the present study at high frequency is similar to that observed in study [13]. However, this increase is more pronounced for 5 wt% loading than in study [13].

At 2 wt% MWNT loading there was a sudden increase in the complex viscosity showing the possibility of a typical rheological percolation between 1 and 2 wt% loading. This could be better understood by plotting complex viscosity versus MWNT loading at low (0.03 rad/s) and high (75.35 rad/s) frequencies, as shown in Fig. 4. It has been observed that at low frequencies, viscosity increase is a strongly nonlinear function of MWNT loading. At high frequency, viscosity is also a nonlinear function of the MWNT loading but this nonlinearity is weak. At the low frequency, there is sharp increase in viscosity at 2 wt% MWNT loading clearly suggesting the existence of a typical rheological percolation between 1 and 2 wt% MWNT loading. This increase in viscosity is more significant in the ultrasonically treated nanocomposites. Evidently, the latter effect is due to the improved dispersion of MWNTs by ultrasonic treatment. The improved dispersion of nanotubes can further be substantiated by the increase in the storage

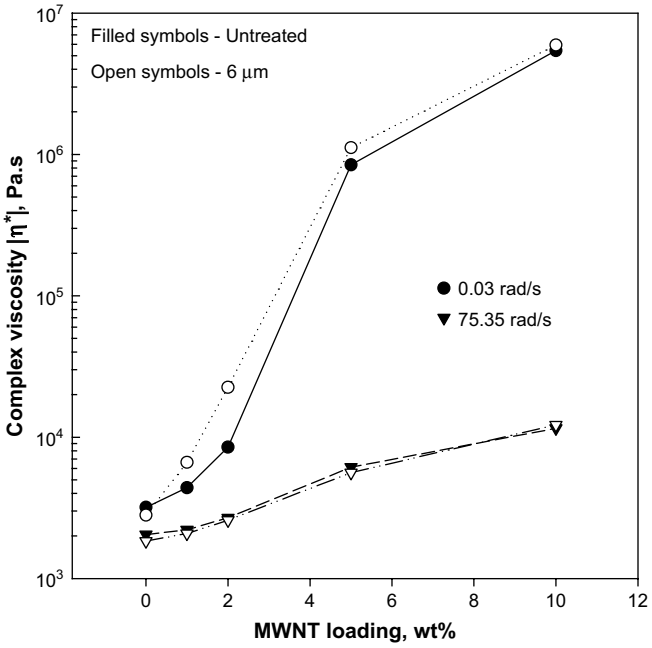

Fig. 4. Complex viscosity versus MWNT loading at frequencies of 0.03 and 75.35 rad/s for untreated and ultrasonically treated nanocomposites at an amplitude of 6 μm.

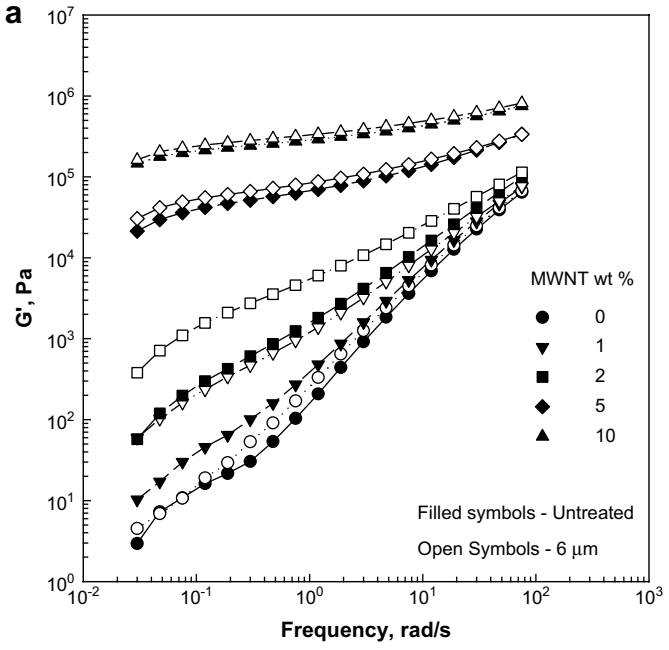

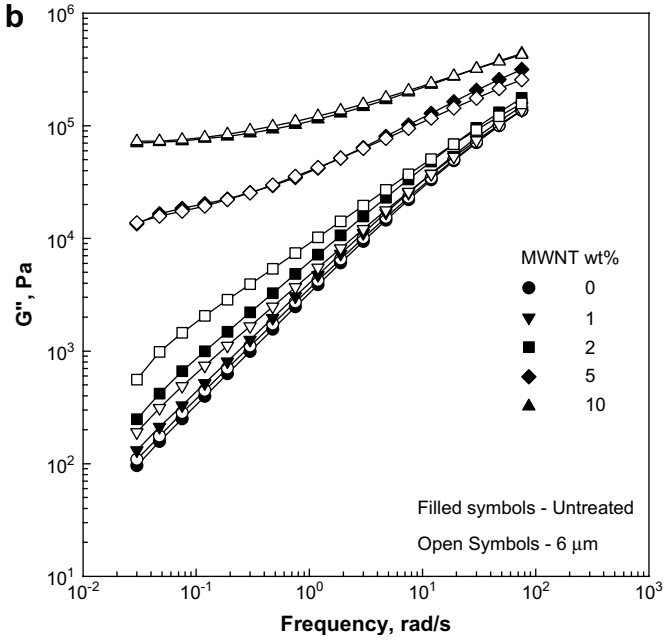

Fig. 5. Storage (a) and loss (b) moduli versus frequency at different MWNT loadings for untreated and ultrasonically treated nanocomposites at an amplitude of 6 μm.

modulus (G'). Both storage (G') and loss (G'') moduli increase with MWNT loadings with a greater increase in G' than G'' (Fig. 5). The storage modulus was increased by many orders of magnitude with the increase of MWNT loading. The value of G' also increases with frequency but the effect is more pronounced at low MWNT loading as compared to high MWNT loading. At higher loadings, the dependence of G' on frequency becomes very weak almost approaching the plateau region. This indicates the existence of solid like behavior of nanocomposites suggesting that the MWNTs cause the restriction of motion of the polymer chains. In other words, microstructure changes occurred in the polymer restricting the long range dynamics of the polymer chains. The terminal behavior disappears with MWNT loadings further suggesting the formation of a nanotube network with enhanced elasticity of the nanocomposites.

The effect of MWNT loadings and ultrasound on the structural differences between polymer and nanocomposites can be seen from the logarithmic plot of G' versus G'' (Fig. 6) which is similar to the Cole–Cole plot [28] used by various researchers [29–31] to study the dynamic mechanical properties of polymers in the melt state. At a given G'' value, the G' increased significantly with nanotube content and is in accordance with the behavior reported for PC–MWNT composites [13]. It was observed that ultrasonic treatment increases G' at given G'' for nanocomposites at all loadings. The increase in the storage modulus with ultrasonic treatment further indicates improved polymer–nanotubes' interaction and better dispersion of MWNTs. The effect of ultrasound and MWNT loading on the damping characteristics of the nanocomposites can be explained by plotting tan δ versus frequency at various MWNT loadings as shown in Fig. 7. It is observed that tan δ decreases with nanotube content. The curve becomes more flat in the low frequency region indicating that the nanotubes strongly affect the relaxation behavior of polymer chains. As can be seen, the storage modulus increases more with ultrasonic treatment than the loss modulus resulting in a lower tan δ value. The decrease in tan δ with MWNT loading is more significant at low frequency than at high frequency. At high loading, the value of tan δ is seen to be higher at high frequency than that at low frequency. But it is opposite at low loadings. In comparison with the untreated samples, the ultrasonically treated nanocomposites show a lower value of tan δ indicating the improved interaction between nanotubes and polymer matrix under action of ultrasound.

3.3. Electrical resistivity

The volume resistivity of nanocomposites as a function of MWNT loading at different ultrasonic amplitudes is plotted in Fig. 8. The volume resistivity decreased by almost 7 orders of magnitude at 10 wt% MWNT loading. A sharp reduction in resistivity was observed at 2 wt% MWNT content indicating that the percolation threshold lies between 1 and 2 wt% MWNT loading. In other words, a critical concentration existed between 1 and 2 wt%

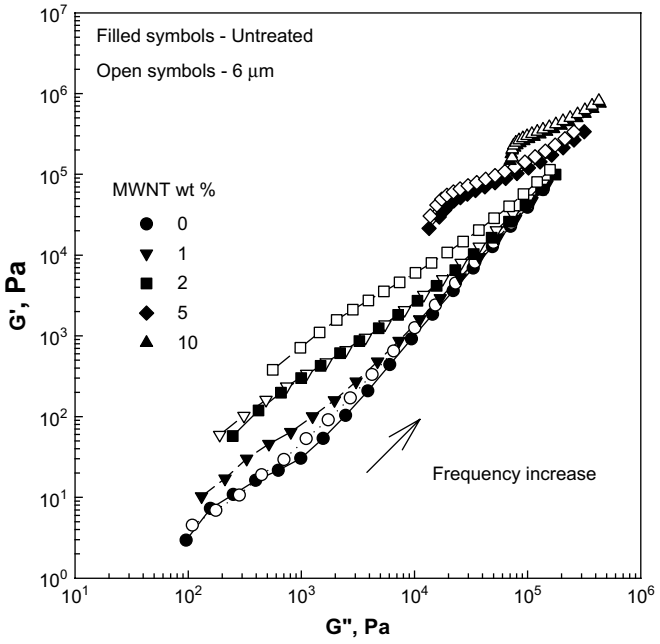

Fig. 6. Storage modulus versus loss modulus at various MWNT loadings for untreated and ultrasonically treated nanocomposites at an amplitude of 6 μm.

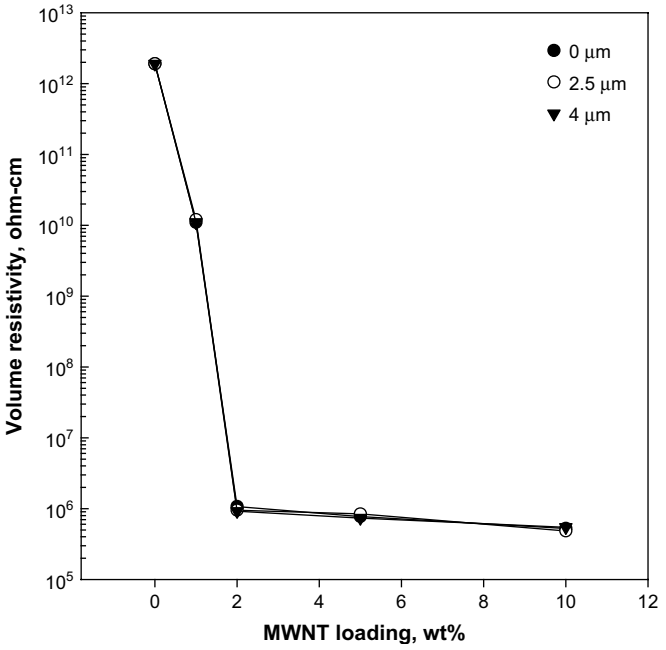

Fig. 8. Volume resistivity as a function of MWNT loading for untreated and ultrasonically treated nanocomposites at various ultrasonic amplitudes.

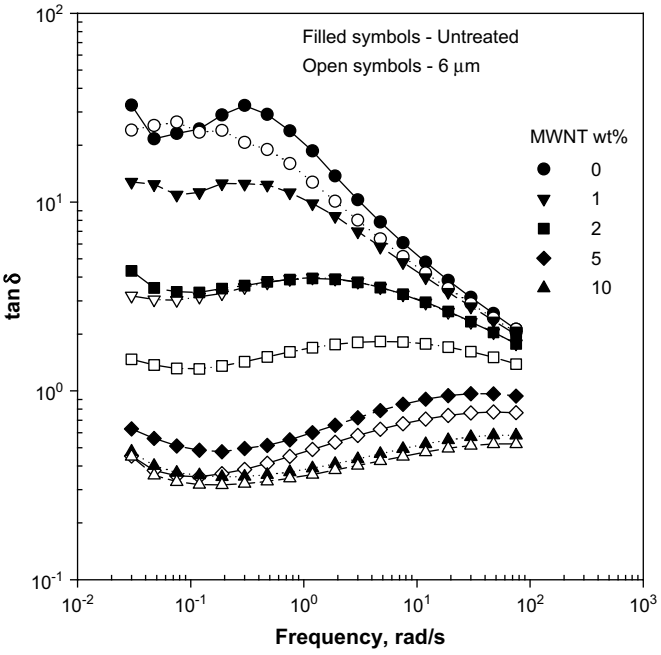

Fig. 7. tan δ versus frequency at various MWNT loadings for untreated and ultrasonically treated nanocomposites at an amplitude of 6 μm.

MWNTs, such that nanotubes form a network resulting in creation of conductive path causing the material to behave like a conductor. These results are in accordance with the percolation threshold reported for PC/MWNT nanocomposites prepared by melt processing method [13]. It has to be noted that all the measurements were done at a constant voltage of 0.1 V. The application of different voltages can lead to different values of resistivity as conductivity shows dependence on applied voltage. At high MWNT loading nonlinear current–voltage behavior was observed [32] due to tunneling mechanism where electron hopping can occur that could change the value of percolation threshold. No significant change in resistivity occurred with further nanotube loading, up to 10 wt%, with ultrasonic treatment. The enhancement of dispersion of nanotubes in ultrasonically treated samples is expected to cause a reduction of number of contacts between the nanotubes, leading to an increase of the resistivity. However, since percolation threshold, where the volume resistivity varies by many orders of magnitude, was already achieved, minor changes in the electrical conductivity due to improved dispersion cannot be detected. Apparently, rheological properties are more sensitive to variation in dispersion of MWNTs than the electrical conductivity.

3.4. Comparison of rheological and electrical percolation

From comparison of Figs. 4 and 8, it was observed that both rheological and electrical percolations are in the same range. At low frequencies a sharp increase in complex viscosity was observed at 2 wt% MWNT loading. This transition is considered as the rheological percolation. Earlier study [13] also reported that electrical and rheological percolation for PC/MWNT composites prepared by melt processing fall in same concentration range of MWNT loading. For PP/MWNT nanocomposites, study [33] indicated that electrical percolation and composite firmness, defined as a reciprocal value of tan δ, were in the concentration range of 0.25–1.0 vol% of MWNTs. In another study [34], PP/CNF composites, prepared by melt processing, showed the same concentration range for both electrical and rheological percolations. In study [15], PE/MWNT composites, also prepared by melt processing method, showed both the rheological and electrical percolations at 7.5 wt% MWNT loading. However, it is interesting to note that in many other studies [35–37], the rheological and electrical percolations were found to be different such that the concentration corresponding to the electrical percolation was higher than that of the rheological percolation. Generally, it is observed that the electrical percolation strongly depends on materials and processing method used. In particular, thermoset materials generally exhibit percolation at lower loading than thermoplastic materials [6,38,39]. Moreover, it was generally observed that concentration corresponding to the percolation increased with the alignment of the CNTs [40]. When CNTs are

aligned, the number of contacts between them is reduced, destroying the CNT network. Therefore, it is difficult to make conductive path at low CNT loading. However, study [41] reported a slight increase in the conductivity with SWNT alignment.

3.5. Mechanical properties

The typical stress–strain curves for the PEI/MWNT nanocomposites at various loadings at constant ultrasonic amplitude of 2.5 μm are shown in Fig. 9. From the figure, one can see that at an amplitude of 2.5 μm the addition of nanotubes does not affect the shape of the stress–strain curves. In particular, the ability of the PEI matrix to exhibit the yielding behavior was retained. This is in contrast to conventional composites that typically become brittle upon addition of fibers.

Young's modulus, tensile strength and yield strain are presented in Fig. 10. The elongation at break was not reported here due to significant scatter in the data. The values are also summarized in Table 1. From Fig. 10, it is observed that the addition of MWNTs has a significant effect on values of the mechanical properties of nanocomposites. In addition, ultrasonic treatment has also some effect on mechanical properties of nanocomposites. Improvement in Young's modulus is seen to be more significant at higher MWNT loading, as seen from Fig. 10(a). In particular, Young's modulus of untreated nanocomposites at 10 wt% MWNT loading is about 70% higher than that of untreated pure PEI. It is also observed that at 10 wt% MWNT loading the nanocomposite treated at an amplitude of 5.0 μm shows 86% increase in Young's modulus, as compared to the untreated PEI matrix. It should be noted that studies [16,42] found a greater improvement in mechanical properties at lower MWNT loadings than at higher loadings possibly due to a lack of dispersion of MWNTs at higher loadings. However, the present study convincingly shows that Young's modulus consistently increased with loading. This implies that dispersion of MWNTs was achieved. As indicated in Fig. 10(b), the tensile strength of the samples increased from 108 MPa for untreated PEI to 115 MPa for PEI nanocomposite at MWNT loading of 10 wt%. A further increase

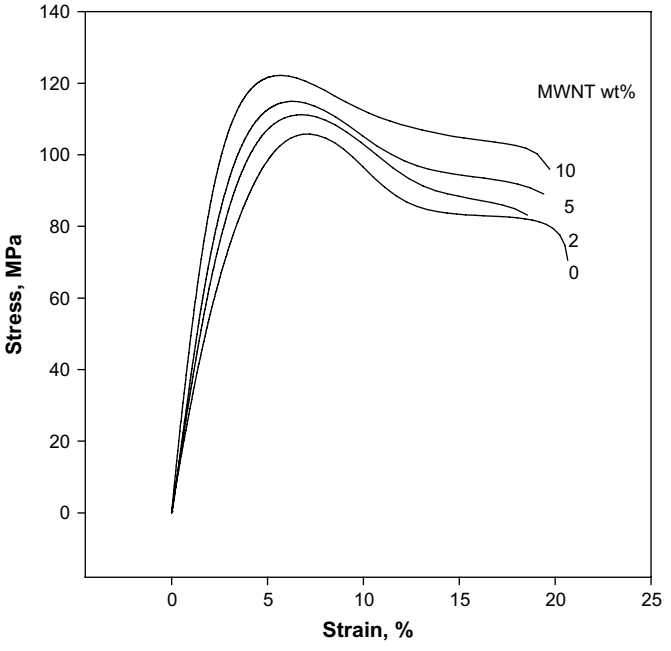

Fig. 9. Typical stress–strain curves of PEI and nanocomposites at various MWNT loadings treated at an ultrasonic amplitude of 2.5 μm.

in the tensile strength was observed for the ultrasonically treated samples. In particular, at an amplitude of 4 μm, the tensile strength increased from 102 MPa for pure PEI to 123 MPa at loading of 10 wt%. The latter clearly indicates that, in addition to a better dispersion of MWNTs, ultrasonic treatment evidently results in increasing the interfacial interactions between polymer matrix and MWNTs. However, for the samples with loadings of 5 and 10 wt%, the tensile strength drops significantly at amplitude greater than 4 μm. This is possibly due to the introduction of defects in both the matrix and the MWNTs under action of high amplitude ultrasonic waves. Fig. 10(c) shows that the yield strain of untreated samples and ultrasonically treated samples at low amplitudes insignificantly affected by MWNT loading. However, the yield strain decreases significantly at high amplitudes due to the introduction of defects in both the matrix and the MWNTs.

Earlier studies indicated that Young's modulus was increased by about 12% for HDPE/MWNT composites at 5 wt% MWNT loading [43], about 19% at 2 wt% MWNT loading for PET/MWNT composites [42] and 30% for PS/MWNT composites at 5 wt% MWNT loading [44]. Contrary to Ref. [43], no significant improvement in mechanical properties was observed for HDPE/MWNT composites [15]. However, the modulus and strength were increased by 50% and 65%, respectively, for HDPE/SWNT composites at 2.6 wt% SWNT loading [45]. Furthermore, a 62% increase in the modulus was obtained for polyamide 6/MWNT composites at 12.5 wt% MWNT loading [46]. In the present study, PEI, being the high performance thermoplastic, exhibits a modulus and strength much higher than those of polymers discussed in this section. However, even in this case a significant increase in both Young's modulus and tensile strength were obtained. This indicates the effectiveness of ultrasonic assisted extrusion developed in the present study. However, it should be noted that the increase of Young's modulus and tensile strength was not large as expected from the composite rule of mixture [47]. A number of ways were suggested to improve the mechanical properties of the nanotube-based nanocomposites. A common method to improve the mechanical properties of the nanocomposites is to provide orientation or alignment to the CNTs. This is commonly done by melt spinning at high draw ratio to make fibers with CNTs oriented along the fiber axis [48]. Studies [49,50] have shown that the increased alignment provides better mechanical properties. However, in those cases CNT concentration corresponding to electrical percolation was higher due to the alignment of CNTs [41]. In study [51], PMMA/SWNT composites were melt spun to make fibers at various draw ratios. A significant improvement in mechanical properties was observed. In addition, Fornes et al. [52] prepared melt spun fibers from PC/MWNT which resulted in the increase in Young's modulus and tensile strength by 75% and 50%, respectively, at 5 wt% MWNT loadings. Also, PP/SWNT [53] fibers were post-drawn after spinning. An increase in the modulus from 6.3 to 9.8 GPa was observed at a loading of 1 wt%. In another study [54], PP/SWNT fibers showed improvement in the modulus from 0.4 to 1.4 GPa, i.e. more than threefold increase in the strength at 5 wt% SWNT loading. In the present study no alignment or stretching was performed and the die section is of constant rectangular cross section without any converging flow. Hence, the observed enhancement of properties in PEI/MWNT nanocomposites is not due to orientation nanotubes. In fact, they are randomly distributed in PEI matrix as indicated by HRSEM pictures reported below. However, providing orientation to MWNTs by stretching is expected to further enhance the mechanical properties of PEI/MWNT nanocomposites.

From many studies [55,56], it has been observed that CNTs cause nucleation resulting in increased crystallinity of the material. Accordingly, it becomes difficult to find whether the increased mechanical properties are due to increased crystallinity or due to the reinforcement effect of nanotubes. However, in the present

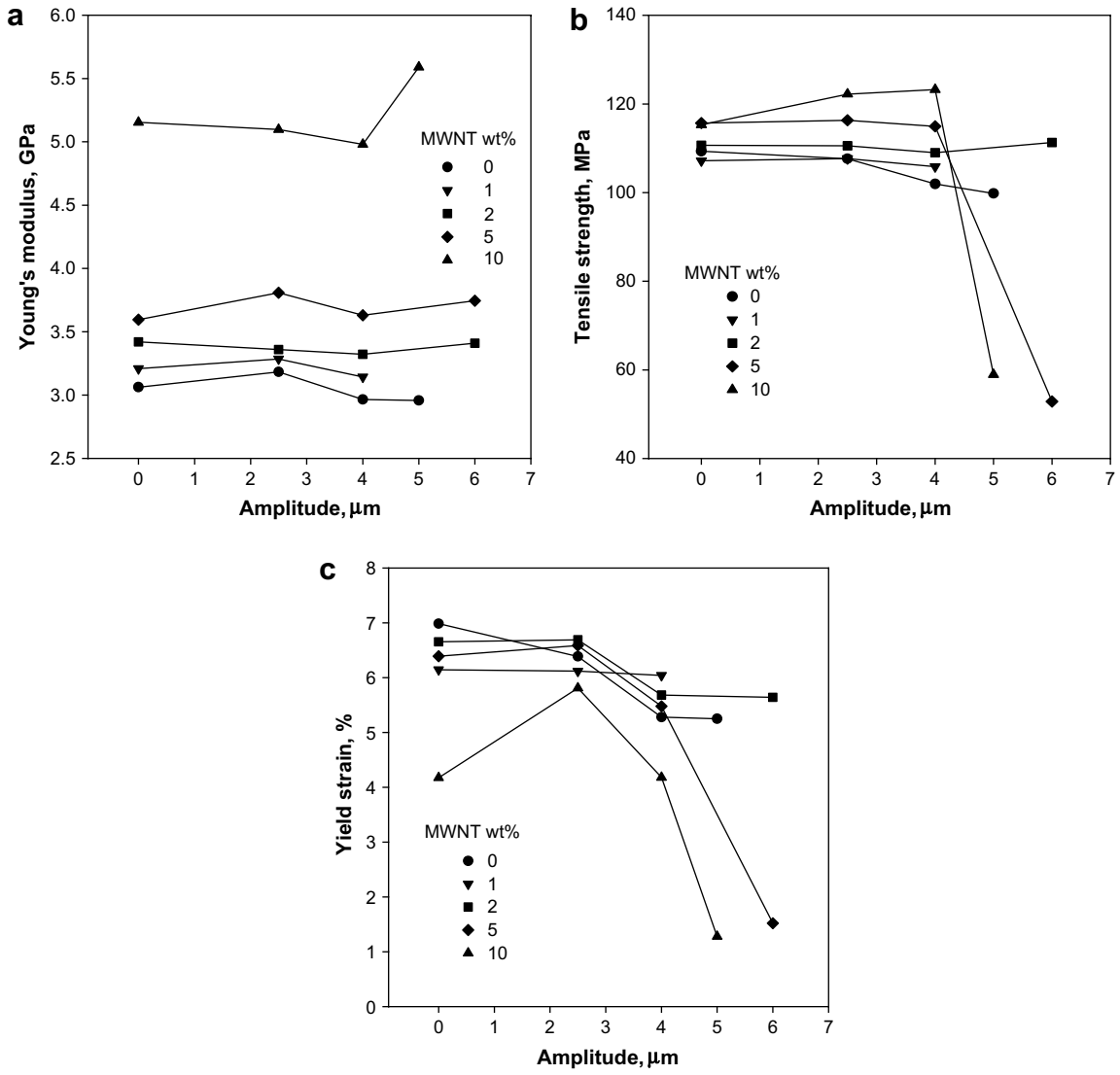

Fig. 10. Young's modulus (a), tensile strength (b) and yield strain (c) versus ultrasonic amplitude for PEI and nanocomposites obtained at different MWNT loadings.

study the polymer matrix, PEI, is an amorphous polymer. Therefore, any improvement in mechanical properties can be attributed to only MWNT reinforcement caused by improved dispersion or increased nanofiller–matrix interactions.

Generally, it is believed that CNTs with larger aspect ratios will yield higher mechanical properties. However, in the case of PC/SWNT fibers Fornes et al. [52] observed little improvement in the mechanical properties above an aspect ratio of 300. At an aspect ratio of ~2000 a further increase in reinforcement was not observed. Another way [57,58] to improve the mechanical properties could be the functionalization of MWNTs to achieve good interaction with the matrix. However, few studies have been carried out to investigate the effect of functionalization on the mechanical properties [59,60].

3.6. Morphology

Fig. 11 shows HRSEM micrographs of surfaces of the as-received MWNTs (a), cryofractured moldings of untreated (b) and ultrasonically treated (c) nanocomposites filled with 2 wt% MWNTs. Image analysis of micrographs of the as-received MWNTs allowed us to determine distribution of their diameters. It was found that their diameters varied from 9 to 28 nm with the average diameter being 18 nm. Images in Fig. 11(b) and (c) clearly distinguish nanotubes that are randomly oriented and uniformly dispersed. However, the untreated nanocomposite sample shows the presence of entangled MWNT bundles as large as 1 μm. Nanotubes in the treated sample were found to be completely unentangled after treatment at an amplitude of 6 μm. This sample does not show even a single MWNT bundle. The images show that the nanotubes were dispersed to a level of 50 nm diameter, which is higher than diameters of 9–28 nm of MWNTs as-received. This suggests that there are two possibilities. First, PEI matrix was coated or wrapped around the MWNTs. This may be a further indication of the existence of interfacial interactions between MWNTs and PEI matrix. Second, the observed increase in diameters of nanotubes could be due to the silver sputter coating used in preparation of the nanocomposite samples for the HRSEM studies. This effect is further explained in detail.

Fig. 12 shows micrographs of the untreated (a, c) and ultrasonically treated (b, d) nanocomposites at 10 wt% MWNT loading and an amplitude of 5.0 μm at low (a, b) and high (c, d) magnifications. Due to very high loading, at low magnification, it is difficult to detect whether dispersion of nanotubes is at the individual level in

Table 1
Mechanical properties of PEI and PEI/MWNT nanocomposites obtained at various ultrasonic amplitudes.

MWNT (wt%)	Ultrasonic amplitude (μm)	Young's modulus (GPa)	Tensile strength (MPa)	Yield strain (%)
0	0	3.06 ± 0.20	109.31 ± 0.6	6.98 ± 0.36
	2.5	3.18 ± 0.09	107.65 ± 1.3	6.71 ± 0.34
	4	2.96 ± 0.40	101.93 ± 4.5	5.5 ± 0.63
	5	2.96 ± 0.21	99.82 ± 0.3	5.25 ± 0.29
1	0	3.21 ± 0.20	107.17 ± 3.9	6.59 ± 0.20
	2.5	3.28 ± 0.20	107.67 ± 1.2	6.12 ± 0.64
	4	3.14 ± 0.14	105.85 ± 4.9	6.59 ± 0.35
2	0	3.42 ± 0.10	110. 67 ± 0.8	6.65 ± 0.18
	2.5	3.36 ± 0.14	110.57 ± 0.4	6.69 ± 0.19
	4	3.32 ± 0.14	109 ± 1.8	6.09 ± 0.95
	6	3.41 ± 0.14	111.29 ± 1.3	6.44 ± 0.60
5	0	3.60 ± 0.20	115.68 ± 0.4	6.39 ± 0.19
	2.5	3.81 ± 0.16	116.31 ± 2.3	6.59 ± 0.27
	4	3.63 ± 0.30	114.95 ± 2.7	5.82 ± 0.84
	6	3.75 ± 0.26	52.87 ± 2.4	1.52 ± 0.05
10	0	5.15 ± 0.65	115.3 ± 6.1	4.86 ± 0.69
	2.5	5.10 ± 0.11	122.21 ± 0.3	5.18 ± 0.09
	4	4.98 ± 0.60	123.24 ± 2.1	5.01 ± 0.69
	5	5.59 ± 1.26	58. 94 ± 4.8	1.17 ± 0.09

both the untreated and the treated samples. However, one can see that the untreated sample shows the resin rich part along with a network of nanotubes, whereas the treated sample seems to indicate dispersed nanotubes forming the network all over the polymer matrix. Another interesting observation can be made about the length of the nanotubes. It has been observed that the treated sample shows longer nanotubes than the untreated one. This can be seen from comparison of Fig. 12(c) and (d) obtained at high magnification. However, why this occurs is not clear. One possible reason could be the tremendous decrease in die pressure with ultrasonic treatment as compared to the untreated samples (see Fig. 2(a)). The lower pressure may lead to a reduction of the breakage of nanotubes.

Fig. 13 shows a typical HRSEM micrograph of ultrasonically treated nanocomposites at a loading of 10 wt% and an amplitude of 5 μm obtained without the silver sputter coating. The image analysis of various micrographs was performed. An interesting observation was made from the comparison of the micrographs that were obtained with (Fig. 12(d)) and without (Fig. 13) the silver sputter coating. Nanotube diameters appear to be bigger with the sputter coating. In particular, nanocomposites without sputter coating show the diameter of nanotubes ranging from 10 to 64 nm with an average diameter of 30 nm. This is a clear indication of PEI matrix getting coated or wrapped around the MWNTs and a further proof of the existence of interfacial interactions between MWNTs and PEI matrix. However, the mechanism of nanotube interaction with polymer matrix is not clear at this stage. Further work needs to be done to understand this phenomenon. At higher MWNT loadings, due to high aspect ratio and large surface area, nanotubes formed an interconnected network.

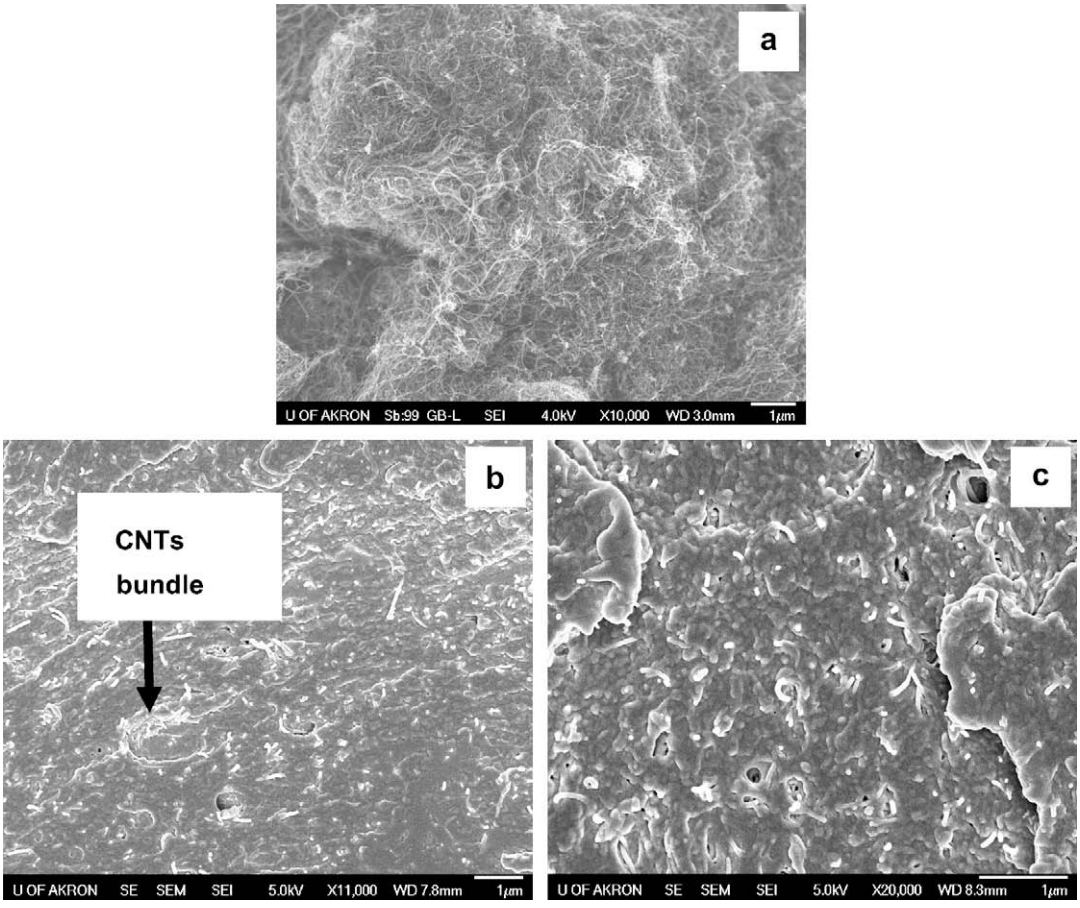

Fig. 11. HRSEM micrographs of as-received MWNTs (a), surface of cryofractured moldings of untreated nanocomposite (b) and ultrasonically treated nanocomposite (c) at 2 wt% MWNT loading and an amplitude of 6 μm.

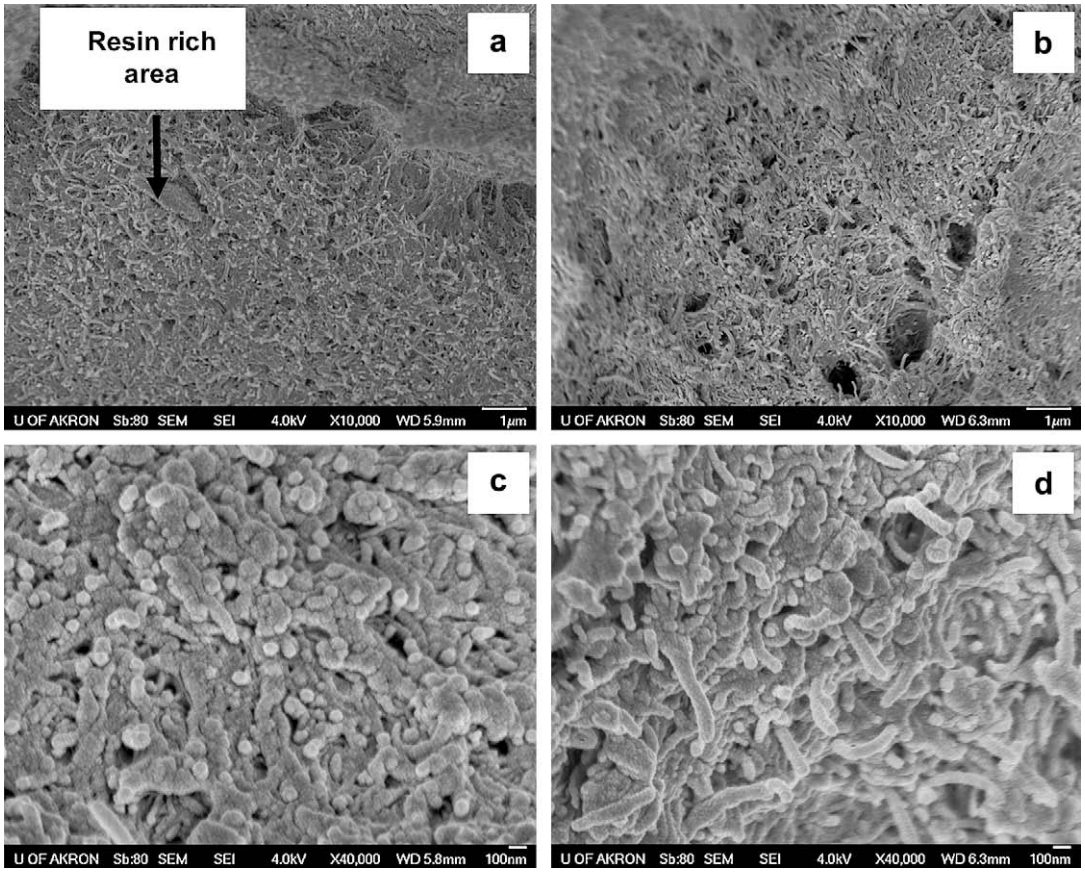

Fig. 12. HRSEM micrographs of sputter-coated surface of cryofractured moldings of untreated (a and c) and ultrasonically treated (b and d) nanocomposites at 10 wt% MWNT loading and an amplitude of 5 μm. (a and b): low magnification; (c and d): high magnification.

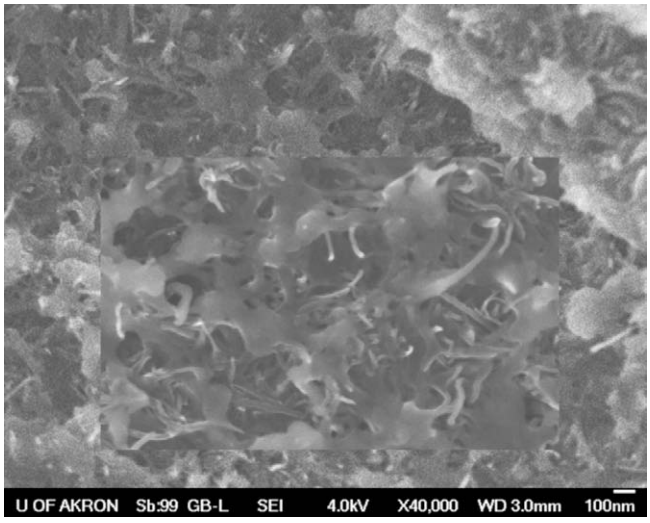

Fig. 13. HRSEM micrograph without sputter coating surface of cryofractured moldings of ultrasonically treated nanocomposites at 10 wt% MWNT loading and an amplitude of 5 μm.

4. Conclusions

A new ultrasound assisted twin screw extrusion process was developed for manufacturing PEI/MWNT nanocomposites with excellent dispersion of nanotubes in a polymer matrix. This process is solvent free and uses no surface modification of the nanotubes. The rheological behavior of the nanocomposites was studied in the oscillatory shear mode. The rheological behavior was considered as an indirect way to determine the dispersion state of MWNTs. The tremendous increase in the complex viscosity and storage modulus of PEI was observed with MWNT loading. In addition, the rheology was affected by ultrasonic treatment. In particular, the ultrasonically treated nanocomposites show an increase in the viscosity, storage modulus and reduced damping characteristics, as compared to the untreated ones. This indirectly indicates the presence of better dispersion of nanotubes in PEI under ultrasonic treatment. At low MWNT loading, the shear thinning behavior of nanocomposites is similar to that of the matrix. At high nanotube loading, nanocomposites show very strong shear thinning behavior. Data on mechanical properties shows that MWNT loading and ultrasound have an effect on the tensile strength and Young's modulus of the nanocomposites. In particular, Young's modulus of the treated nanocomposites shows some increase in values at loadings of 5 and 10 wt%. Also, the strength of nanocomposites increased from 115 MPa for the untreated sample to 123 MPa for the treated sample at 10 wt% MWNT loading and amplitudes of 2.5 and 4 μm. However, reductions in the tensile strength and yield strain were observed in nanocomposites treated at higher amplitudes. The rheological and electrical percolations were found to be between 1 and 2 wt% MWNT loading. Rheology was found to be more sensitive to MWNT dispersion than the electrical conductivity. HRSEM results show that ultrasound helps in dispersion of nanotubes as a result of breakage of MWNT bundles.

Acknowledgements

The authors are grateful for the financial support provided by NSF under Grant No. CMMI-0654326 and NASA Headquarters.

References

[1] Thostenson ET, Ren Z, Chou TW. Compos Sci Technol 2001;61:1899.
[2] Oberlin A, Endo M, Koyama T. J Cryst Growth 1976;32:335.
[3] Iijima S. Nature 1991;354:56.
[4] Breuer O, Sundararaj U. Polym Compos 2004;25(6):630.
[5] Ajayan PM. Chem Rev 1999;99:1787.
[6] Sandler J, Shaffer MSP, Prasse T, Bauhofer W, Schulte K, Windle AH. Polymer 1999;40:5967.
[7] Liu P. Eur Polym J 2005;41:2693.
[8] Park C, Ounaies Z, Watson KA, Crooks RE, Smith J, Lowther SE, et al. Chem Phys Lett 2002;364:303.
[9] Hilding J, Grulke EA, Zhang ZG, Lockwood F. J Dispersion Sci Technol 2003;24(1):1.
[10] Xie XL, Mai YW, Zhou XP. Mater Sci Eng R 2005;49:89.
[11] Lu KL, Lago RM, Chen YK, Green MLH, Harris PJF, Tsang SC. Carbon 1996;34(6):814.
[12] Jin Z, Pramoda KP, Xu G, Goh SH. Chem Phys Lett 2001;337:43.
[13] Potschke P, Fornes TD, Paul DR. Polymer 2002;43:3247.
[14] Potschke P, Bhattacharyya AR, Janke A. Eur Polym J 2004;40:137.
[15] McNally T, Potschke P, Halley P, Murphy M, Martin D, Bell SEJ, et al. Polymer 2005;46:8222.
[16] Chen GX, Kim HS, Park BH, Yoon JS. Polymer 2006;47:4760.
[17] Siochi EJ, Working DC, Park C, Lillehei PT, Rouse JH, Topping CC, et al. Composites Part B 2004;35:439.
[18] Isayev AI, Wong CM, Zeng X. Adv Polym Technol 1990;10:31.
[19] Isayev AI, Chen J. US Patent 5,284,625; 1994.
[20] Isayev AI, Chen J, Tukachinsky A. Rubber Chem Technol 1995;68:267.
[21] Isayev AI, Yushanov SP, Chen J. J Appl Polym Sci 1996;59:815.
[22] Tukachinsky A, Schworm D, Isayev AI. Rubber Chem Technol 1996;69:92.
[23] Feng W, Isayev AI. Polymer 2004;45:1207.
[24] Lapshin S, Isayev AI. J Vinyl Additive Technol 2006;12:78.
[25] Krishnamorti R, Vaia RA, Giannelis EP. Chem Mater 1996;8:1728.
[26] Hyun YH, Lim ST, Choi HJ, Jhon MS. Macromolecules 2001;34:8084.
[27] Solomon MJ, Almusallam AS, Seefeldt KF, Somwangthanaroj A, Varadan P. Macromolecules 2001;34:1864.
[28] Cole KS, Cole RH. J Chem Phys 1941;9:341.
[29] Kanakkanatt SV. J Cell Plast 1973;9:54.
[30] Han CD, Kim J, Kim JK. Macromolecules 1989;22:383.
[31] Chuang HK, Han CD. J Appl Polym Sci 1984;29:2205.
[32] Ounaies Z, Park C, Wise KE, Siochi EJ, Harrison JS. Compos Sci Technol 2003;63:1637.
[33] Kharchenko SB, Douglas JK, Obrzut J, Grulke EA, Migler KB. Nat Mater 2004;3:564.
[34] Lozano K, Bonilla-Rios J, Barrera EV. J Appl Polym Sci 2001;80:1162.
[35] Hu G, Zhao C, Zhang S, Yang M, Wang Z. Polymer 2006;47:480.
[36] Du F, Scogna RC, Zhou W, Brand S, Fischer JE, Winey KI. Macromolecules 2004;37:9048.
[37] Potschke P, Abdel-Goad M, Alig I, Dudkin S, Lellinger D. Polymer 2004;45:8863.
[38] Pecastaings G, Delhaes P, Derre A, Saadaoui H, Carmona F, Cui S. J Nanosci Nanotechnol 2004;46:877.
[39] Martin CA, Sandler JKW, Windle AH, Schwarz MK, Bauhoffer W, Schulte K. Polymer 2005;46:877.
[40] Du F, Fischer JE, Winey KI. Phys Rev B 2005;72. 121404(R).
[41] Choi ES, Brooks JS, Eaton DL, Al-Haik MS, Hussaini MY, Garmestani H, et al. J Appl Phys 2003;94(9):6034.
[42] Kim JY, Park SH, Kim SH. J Appl Polym Sci 2007;103:1450.
[43] Tang W, Santare MH, Advani SG. Carbon 2003;41:2779.
[44] Andrews R, Jacques D, Qian DL, Rantell T. Acc Chem Res 2002;35(12):1008.
[45] Zhang Q, Rastogi S, Chen D, Lippits D, Lemstra PJ. Carbon 2006;44:778.
[46] Menicke O, Kaempfer D, Weickmann H, Friedrich C, Vathauer M, Warth H. Polymer 2004;45(3):739.
[47] Callister WD. Materials science and engineering, an introduction. New York: Wiley; 2003.
[48] Sandler JKW, Pegel S, Cadek M, Gojny F, Van Es M, Lohmar J. Polymer 2004;45(6):2001.
[49] Chae HG, Sreekumar TV, Uchida T, Kumar S. Polymer 2005;46:10925.
[50] Moore EM, Ortiz DL, Marla VT, Shambaugh RL, Grady BP. J Appl Polym Sci 2004;93(6):2926.
[51] Haggenmueller R, Gommans HH, Rinzler AG, Fischer JE, Winey KI. Chem Phys Lett 2003;330(3–4):219.
[52] Fornes TD, Baur JW, Sabba Y, Thomas EL. Polymer 2006;47:1704.
[53] Kearns JC, Shambaugh RL. J Apply Polym Sci 2002;86(8):2079.
[54] Chang TE, Jensen LR, Kisliuk A, Pipes RB, Pyrz R, Sokolov AP. Polymer 2005;46(2):439.
[55] Bhattacharyya AR, Sreekumar TV, Liu T, Kumar S, Ericson LM, Hauge RH, et al. Polymer 2003;44:2373.
[56] Ryan KP, Cadek M, Nicolosi V, Walker S, Reuther M, Fonseca A, et al. Synth Met 2006;156:332.
[57] Bhattacharyya S, Sinturel C, Salvetat JP, Saboungi ML. Appl Phys Lett 2005;86(1):113104.
[58] Yang J, Hu J, Wang C, Qin Y, Guo Z. Macromol Mater Eng 2004;289(9):828.
[59] Xu M, Zhang T, Gu B, Wu J, Chen Q. Macromolecules 2006;36:3540.
[60] Liu L, Barber AH, Nuriel S, Wagner HD. Adv Funct Mater 2005;15(6):975.